American Society of Mechanical Engineers

ASME Accepted Manuscript Repository

Institutional Repository Cover Sheet

Cranfield Collection of E-Research - CERES

ASME Paper Title: Comparative assessment of fouling scenarios in an axial flow compressor

Authors: Ioannis Templalexis, Vassilios Pachidis, Hasani Azamar

ASME Journal Title: Journal of Engineering for Gas Turbines and Power

Volume/Issue: Volume 143, Issue 8 Date of Publication (VOR* Online): 5 December 2020

ASME Digital Collection URL: https://asmedigitalcollection.asme.org/gasturbinespower/article/doi/10.1115/1.4049264/1091912/Comparative-Assessment-of-Fouling-Scenarios-in-an

DOI: https://doi.org/10.1115/1.4049264

*VOR (version of record)

Journal of Engineering for Gas Turbines and Power. Received August 28, 2020;
Accepted manuscript posted December 5, 2020. doi:10.1115/1.4049264
Copyright (c) 2020 by ASME
Journal of Engineering for Gas Turbines and Power
Volume 143, Issue 8, August 2021

Comparative Assessment of Fouling Scenarios in an Axial Flow Compressor

Name, first author[1] Ioannis Templalexis
Affiliation: Associate Professor
Full Mailing Address: Hellenic Air Force Academy, Department of Aeronautical Sciences, Division of Thermodynamics, Propulsion and Power Systems, Dekeleia Air Base - Attiki, Athens - 13671 (1010) – Greece
e-mail: ioannis.templalexis@hafa.haf.gr

Name, second author: Vasilios Pachidis
Affiliation: Professor, Director, Rolls-Royce UTC in Aero Systems Design, Integration & Performance
Full Mailing Address: School of Aerospace, Transport and Manufacturing Building 52, Room 334, Cranfield University, Bedfordshire, MK43 0AL
e-mail: v.pachidis@cranfield.ac.uk

Name, third author: Hasani Azamar Aguirre
Affiliation Research Fellow
Full Mailing Address: Gas Turbine Engineering Group – Centre for Propulsion School Of Aerospace, Transport and Manufacturing UTC Rolls-Royce Office 213, Whittle Building (52) Cranfield University, Cranfield, Bedfordshire MK43 0AL, United Kingdom
e-mail: h.azamaraguirre@cranfield.ac.uk

ABSTRACT

It is commonly accepted that fouling degrades severely axial compressor performance. Deposits build up as operating hours sum up, causing a decrease in the compressor's delivery pressure, efficiency and flow capacity. Compressor susceptibility to fouling depends on many factors, such as atmospheric conditions, air quality, filtration system, the size and design of the compressor, etc. The current study identifies four basic operating scenarios which refer to the same compressor, in order to put forward a comparative assessment as to how incoming air quality would affect compressor performance. SOCRATES, an in-house, streamline curvature-based through-flow tool, in conjunction with a detailed, fully customizable fouling

[1] Associate Professor Ioannis Templalexis.

Published by The American Society of Mechanical Engineers. This is the Author Accepted Manuscript issued with:
Creative Commons Attribution License (CC BY). The final published version is available online at DOI:https://doi.org/10.1115/1.4049264.
Please refer to any applicable publisher terms of use.

empirical model, conceived based on flow physics and relevant experimental data, is used to qualify and quantify, compressor degradation with time.

INTRODUCTION

The starting point for the current research, was the basic conclusion drawn by Kurz et al. [1]: The presence of wet contaminants and/or high air humidity and the quality of air filtration systems, have a far greater impact on fouling rates, than engine specific fouling susceptibility factors. The size of airborne particles ingested into the engine is primarily controlled by the presence of a filtration system. On the other hand, the particle deposition rate and the fouling patterns formed on the blade surfaces are greatly affected by the "stickiness" of the blade surfaces which in turn is affected by the moisture level of the incoming air. Compressor geometry, size and operating point would affect far less the rate of contaminants built up on the wetted surfaces and they would affect even less the exact location on compressor walls and blade surfaces.

The current study identifies four basic operating scenarios which refer to the same compressor, in order to put forward a comparative assessment as to how the factors mentioned above, affect the compressor performance through the fouling mechanism. Scenarios were formed out of the possible combinations regarding the presence of a filtration system and the level of humidity. These were: i) Filtered - dry air, ii) Filtered - humid air, iii) Unfiltered - dry air, and iv) Unfiltered - humid air. These scenarios will eventually reproduce four completely different situations regarding the quality of the incoming air and subsequently, four different fouling regimes for the compressor operating downstream. Data to support the impact of each reported

incoming air condition on compressor wetted surfaces, are based on experimental findings collected from a thorough literature review. A fixed operating period was set for all cases. In the absence of on-line washing installed on the compressor, this period was set equal to a typical time interval between two consecutive offline washes.

Prescribed requirements of the computational tool selected to build the compressor model were: i) low computational power since several runs have to be performed in order to cover the assumed time period and ii) ability to introduce the imprint of various fouling patterns on compressor blades, into the performance of the compressor. SOCRATES, an in-house two-dimensional, streamline curvature-based, through-flow computational tool, meets these requirements and it was used for this study. A fully customizable empirical model, recently introduced in the code, takes into account various aspects of fouling such as the surface roughness level, the flow blockage and the altered deviation angle at the exit of the blade row. A coverage factor was introduced which takes into account the location and the extent of fouling onto the blade surfaces.

The manuscript is structured as follows: Firstly, a literature review is given, related to compressor fouling. Research is specially focused on the underlying mechanisms and simulation efforts done by researchers during the past. Then the simulation tool is presented along with the empirical fouling model update. Within the section that follows, the four fouling scenarios are thoroughly described and justified based on the criteria upon which their definition was based. Finally, before summarizing

the basic findings and conclusions, the comparative results between the four scenarios are presented.

LITERATURE REVIEW

Compressor fouling, as an engine fault, refers to the performance degradation of the compressor caused by deposit built up on the wetted surfaces. Deposits affect the performance of the compressor since they: i) increase the surface roughness, and ii) alter the gas path geometry. The aforementioned events will lead to compressor performance degradation. Schneider [3] in terms of specific performance parameters, tracks down a reduction in all isentropic efficiency, swallowing capacity and pressure ratio. The fact that deposits are to a certain extent removable, put compressor washing in the center of interest for many researchers and users. There is a lot of relevant published research on compressor washing. Boyce et al. [4] conducted a series of onsite tests on several installed gas turbine engines, as part of their effort to define an optimum, universal washing schedule. They concluded that an optimum washing schedule does exist, but it is case specific as it depends among others, on the site location. Brun et al. [5] gives a good literature review on similar attempts to optimize a combination of offline and online washing schedules. Aretakis et al. [6] coupled an economic model along with their engine performance model and explored the impact of several factors on the formation of an optimal washing schedule. Stalder et al. [7] revealed the importance of humidity content of the incoming air on the fouling process. He noticed, based on onsite measurements that the power loss maximizes at a certain value of total absolute humidity. The power loss increases as long as the water content

functions as a sticking agent for the contaminants and decreases when the water content surpasses a limiting value functioning as a washing medium for the compressor. There have also been several studies addressing the type and extent of fouling occurring based on the engine size [8], the particle size [9] and the composition of incoming air contaminants [10]. In the later researchers looked, at the impact of compressor fouling caused when there is high sea water content in the stream of the incoming air. A good summary of particle entrainment and deposition mechanisms is given in [11]. Finally, as far as the impact of fouling on compressor performance and the entire engine performance is concerned, the reader can find several references in the open literature. Aker et al. [12] and Diakunchak et al. [13] were among the pioneers in this field. Meher-Homji et al. [14] provided a good summary of relevant work.

SIMULATION TOOL

The four fouling scenarios were reproduced using a compressor model build in SOCRATES, a Cranfield University in-house through-flow simulation tool. The tool was first introduced in 2007 [15]. It is based on a through-flow method (Streamline Curvature SLC). The SLC method solves the radial equilibrium equation (REE) to determine the gradient of the meridional velocity spanwise at the intersections between the streamlines and the blade rows. The viscosity effects present in the flow are introduced through empirical models which are based on standard blade profiles. The calculation procedure embedded in the computational tool, is described thoroughly in [18]. The numerical solver is based on a series of nested loops which for a target mass flow or exit static pressure value, a guessed distribution of meridional velocity

distribution across the blade leading and trailing edges is continuously updated until each streamtube conveys the correct amount of mass per unit time. There are several publications focusing on different aspects of the code, such as an innovative loss model adaptation technique [16], integration with 0-D tools [17, 18], a thorough study on the importance of the force terms modelling in the radial equilibrium equation [19], and most recently the prediction of losses from calculated shock wave patterns [33] and compressor performance in choking conditions. [34].

The fidelity level of the flow solution is mainly dependent upon the set of phenomelogical models incorporated in the solution code, which are there to account for the flow viscosity related effects. The inviscid flow calculation of the flow solver for the geometry used in the current study was tested using the values for the loss factors (profile and shock loss), blockage factors and deviation angles reported in [2]. According to [19], the same validation study was conducted on a similar geometry [32]. Both studies confirmed that the inviscid flow component is calculated correctly and also that all the "side effects" caused by entropy generation, are correctly accounted for, through the introduction of appropriate body forces [19].

EMPIRICAL MODEL

In [2] a thorough description is given of a novel fouling loss model which was conceived in order to address the effect of compressor fouling on the induced profile loses, flow blockage and deviation angle. The model was validated against the high fidelity, CFD numerical results obtained by Morini et al. [20]. This comparison showed that the model is capturing correctly the qualitative trends across the operating mass flow range tested,

a fact that makes it appropriate to be used for comparative studies like the one presented in the current manuscript. The initial version of the fouling model did not take into account the degree of coverage and the location of the deposits on the blade surfaces. In the paragraphs that follow, each component of the empirical model is briefly presented, along with the modifications which account for the location and the extent of coverage.

Profile Loss Model

The model which accounts for profile losses [2] is based on a Moodi's type of diagram, as defined by Koch and Smith [21] with some modifications in order to incorporate the dependence of profile losses on surface roughness increase caused by the blade deposits, at various Reynolds number levels. The model was built based on relevant experimental work done by Morini [20]. The model was defined on the principle that the total profile loss consists of two components: the basic profile loss and the fouling profile loss corresponding to the clean and fouled blade performance respectively (equation 1). Each of these components is further split into their corresponding minimum profile loss and off-design loss subcomponents (equations 2 and 3). The minimum profile loss occurs at the minimum loss incidence conditions. Any other incidence angle setting will cause additional profile loss for the flow, which is accounted by the off-design profile loss components.

Seung et al, [22] conducted a systematic experimental work to investigate, among others, the impact of deposit location on the compressor performance. The aforementioned fouling profile loss model was modified accordingly, based on these experimental results, in order to take into account, the degree of coverage and the

location of the deposits. A coverage factor was defined which practically interprets the loss versus Reynolds number curves shown in figure 13 of [22].

The existing fouling loss model corresponds to the full roughened case. It can be seen that for the case of roughened pressure side and a roughened leading edge the profile loss has very little dependency on Reynolds number. Similarly, for the case where the suction side is covered with fouling deposits up to 20%, the profile loss still has no dependence on Reynolds number. Consequently, the "Coverage Factor" needs to address the dependence of the profile loss on the Reynolds number for various deposit locations around the blade surfaces only in the case where fouling exists on the suction side at a coverage percentage between 20% and 100%. In particular, in case of 100% fouled suction side, the profile loss starts to increase exponentially for Reynolds number values over 5,5 10^5, in case of 50% fouled suction side, the exponential increase starts for Reynolds number values over 6 10^5 and lastly in case of 35% fouled suction side the corresponding increase starts for Reynolds number values over 6,5 10^5. These refer to a certain incidence angle and therefore the effect of blade coverage is taken into account for the calculation of the minimum profile loss factor. In other words, it is considered that the entire pressure loss vs. incidence angle curve is shifted without a change occurring on its shape. Based on the proposed profile loss model the total profile loss factor comes as a sum of the basic profile loss component which refers to the clean blade surface plus the fouling related component. Each of these is further decomposed into their corresponding minimum loss and off-design components:

$$\omega_{p,total} = \omega_{p,basic} + \omega_{\mathrm{p,fouling}} \quad (1)$$

where

$$\omega_{p,basic} = \omega_{p,basic,ml} + \omega_{p,basic,OD} \quad (2)$$

$$\omega_{p,fouling} = \omega_{p,fouling,ml} + \omega_{p,fouling,OD} \quad (3)$$

The first term on the RHS of equation 1, the basic profile loss component, is calculated as described in [23]. The method is presented also in [2]. The second term on the RHS of equation 1, expresses flow irreversibilities due to fouling and it is determined based on the Reynolds number level and the relative surface roughness increase caused by the blade deposits. The minimum loss component in equation 3, is determined for the case where air is coming at minimum loss incidence and the blade is fully covered with deposits resulting in a uniform surface roughness increase at every blade location. Therefore, minimum fouling profile loss factor values, as defined above, correspond to the 100% roughened blade. Consequently, the coverage factor shall be defined in a way to reduce the fouling minimum profile loss factor, for any other case where the blade is not fully covered with deposits. Based on the above, equation (4) gives the minimum fouling profile factor taking also into account the degree of coverage:

$$\omega_{p,fouling,ml,cf} = CF * \omega_{p,fouling,ml} \quad (4)$$

where CF takes values between 0 and 1 and equals to zero when the extent of fouling does not affect the profile losses. The off-design fouling loss component will also be equal to zero, since it is determined based on its corresponding minimum loss value.

Deviation Model

It is generally accepted that the deviation angle increases with increasing surface roughness [24], [25], [26]. The current fouling loss model as far as the deviation angle

change is concerned, adopts the method reported in [24]. The results refer to 100% covered blade surface. Based on the literature search conducted by the authors, there were no publicly available experimental or even computational results on the effect of the fouling location on the deviation angle change. However, according to the static pressure distributions shown in figure 10 of [22], (i.e. the static pressure distribution curves correspond to the loss vs Reynolds number curves that were used to define the coverage factor in section 4.1) the static pressure coefficient changes considerably only for the cases of 100% “suction side roughened blade” and "entirely roughened blade”. Static pressure distribution around the airfoil gives an indication of the blade loading and at a constant incidence angle a change in blade loading can only come from a change in the deviation angle. Therefore, the approach adopted for this study was that the deviation angle component due to fouling will only be considered in the cases where at least one side, the entire suction surface, is covered with fouling deposits.

Blockage

The existing fouling model considers that additional flow blockage is introduced to the flow, through both the thickening of the blade profile and the thickening of the boundary layer. Regarding the first, direct mechanism of flow restriction, the current version of the through-flow computational tool used, would only "sense" a change in the blade profile shape through the change in the cascade throat area. Since the geometry and the fouling pattern are fully defined in the input file, in terms of location and deposit layer thickness, no further changes were necessary for the geometrical calculations.

For the second, indirect blockage mechanism, the boundary layer thickening induced blockage, the existing model is based on the calculated total profile loss factor. A value for the equivalent diffusion factor is determined for a certain profile loss factor value, which is then used to determine the blockage factor value. Consequently, as in the case of geometrical changes, the current model adopts without further modifications, the effect of fouling location on the induced blockage.

SCENARIO DEFINITION

Compressor fouling is a process controlled by many factors. It depends on the condition of the incoming air, the design of the engine in general and the compressor itself, and the engine operating point. It is therefore highly improbable, and it has not been done yet, to establish a universally applicable methodology, based on which one could predict the exact fouling pattern and subsequently the effect of this pattern on compressor performance. However, there have been numerous attempts to predict the rate and the degree of fouling taking into account the above-mentioned factors. In the current study, authors defined operating scenarios, applied on the same compressor, in order to reveal the effect of the filtration system and the moisture of the incoming air, onto the compressor performance. Specifically, four scenarios were defined: i) Dry filtered air, ii) Wet filtered air, iii) Dry unfiltered air, and iv) Wet unfiltered air. The expected compressor fouling condition assumed (and described later on in this section for each fouling scenario) was based on the following remarks:

i. The presence of a filter in the incoming air, blocks a certain percentage of the higher diameter airborne particles. The limiting, smallest particle diameter that the filter blocks, depends obviously on the type of filter.

ii. The higher the particle diameter the easier for it to deviate from the streamline path and follow its inertial trajectory. On the other hand, smaller particles abide to the diffusion, contamination mechanisms. These follow in general the streamline path and they tend to end up on the suction surface of the blade, especially in areas of high turbulence intensity.

iii. Based on remarks by Kurz [1], most particles would reach the pressure surface of a blade rather than the suction, through inertial impact. Collection efficiency for inertial impaction, maximizes for high particle diameter.

iv. The presence of moisture and the nature of the particles will primarily affect the built-up rate of the contaminants.

v. Experiments carried out by Seug [22], have shown that fouling implications on compressor performance aggravate when the suction surface, as compared to the pressure surface, is fouled.

When a filter is installed in the intake, only the smaller diameter particles will be let into the compressor. These particles according to point (ii), when entrained by the air, will follow the streamline paths closely and they will most probably depose on the suction surface of the blades and in particular in areas of high turbulence intensity. Consequently, the compressor blades, in the case of the first scenario, are expected to operate with a percentage of their suction surface covered with deposits. In the case

where the air is humid, (2nd scenario) particles will in general still be entrained along the streamline paths and deposits will appear in the same locations, at a higher built up rate. On the other hand, when the compressor is ingesting dry atmospheric air unfiltered, the entrainment mechanism, which refers to the small particles as described in the first scenario, will be present, but according to points ii and iii , the pressure surface of the blade will also be covered with deposits. In other words, the third scenario will result in fully fouled blades. Finally, in the case of the fourth scenario according to which the air has a high humidity content, or the particles are of sticky nature, the blades will be covered with deposits faster than in the third scenario.

The axial flow fan "NASA Stage 37" was selected for the assessment of the proposed case studies. Design and performance data can be found in [27]. It is a single stage axial fan fitted with an inlet and exhaust duct. The rotor has 36 blades, of MCA profile, characterized by an inlet hub to tip diameter ratio of 0.7, a blade aspect ratio of 1.19 and a tip solidity of 1.29. The stator has 46 blades with an aspect ratio of 1.26 and a tip solidity of 1.3. The stage performance is summarized in table 1.

The aforementioned geometry was selected by the research team to demonstrate the validity of their model, for the following reasons:

a) A single-stage geometry is enough to conduct a comparative study between the four scenarios.

b) The same geometry was used by the authors to test the validity of the underlying set of fouling loss models [2]. Given the fact that there are no relevant data to validate

directly the proposed fouling scenarios, the current geometry presents a good starting point for such a study.

The inputs for each scenario are summarized in table 2. Given the fact that the compressor is not linked to a gas turbine engine, its performance is quantified on the basis of total enthalpy rise. A typical TBO of 1000 hours was considered, split in five, two hundred hours-long operating periods. Input for the 1st scenario (Dry unfiltered air) was based on [28], figure 9 where the equivalent sand grain roughness increase due to fouling depositions, is related to the number of operating hours, for Stage 37. In this study roughness was considered uniform along the entire surface of the rotor and the stator blades. This data was adopted because first they refer to the same geometry, and second, as it was explained above, in the case of unfiltered dry operation, blades are considered to get fully fouled, with progressively increasing roughness. In the case where a filter is installed, the blade is considered to be covered by 60% at all times, a percentage which roughly corresponds to the blade area percentage where high turbulence intensity exists. Based on Suman et al. [29], deposits on the suction surface appear distributed on the whole blade surface. The same conditions were assumed along the entire blade span in this study. The rate of roughness increase vs. operating time was kept the same, since the filter will only block the higher diameter particles which are generally guided towards the pressure surface. The 2nd and 4th scenarios generally represent an operating environment where enhanced "sticking conditions" are present. This can be caused for instance by oil mist concentrations, high humidity air and by the nature of the contaminants itself. The aforementioned conditions compared

to the 1st and 3rd scenarios, will mainly affect the rate of deposition and much less the areas where contaminants are deposited. Empirical correlations derived from Vigueras' [30] experimental work was used to determine the surface roughness increase rate for these two scenarios. Vigueras, in his axial compression stage test rig, examined the fouling behavior of the stage when blades are covered with a sticking agent. He measured and defined a series of empirical equations, regarding area specific surface roughness variation. An average surface roughness variation rate, based on these empirical equations, was adopted for the two remaining scenarios. The time scale had to be adapted to the conditions of the case study. The test rig fouling rate, that is the mass rate of contaminants entrained into the compressor, was 100 gr/h. In order to retain consistency between the four scenarios, it was assumed that the compressor in the current research work is operating in an environment like the environment where the experimental measurements of Tarabrin [8] were taken. It is reminded that Morini's et al. [28] relative roughness distributions used for the dry air scenarios were derived based on Tarabrin's [8] experimental data. In such an environment the dust concentration according to Giampaolo [31] is 0.06 gr/m^3. The volume rate of the case study compressor is 16.7 [m^3/s], therefore the contaminant ingestion rate equals to 2.8 10^{-5} [kg/s]. On the other hand, the equivalent contaminant ingestion rate for the experimental device, if it had a mass flow equal to the case study compressor would be 4.01 10^{-4} [kg/s]. Comparing the two contaminant ingestion rates, a scaling factor is defined in order to adjust the time scale used in the experiment to the time scale of the case study.

RESULTS AND DISCUSSION

The current study has two major goals:

i) to examine the effect of moisture and air filtering on gas turbine engine compressor performance degradation due to fouling and,

ii) to present an integrated fouling model which in conjunction with a through-flow code and a gas turbine engine performance simulation tool, could substitute the methodology used so far in similar studies, where scaling factors of basic performance parameters are plugged in compressor stage-stacking methods.

The study focuses on the compressor, however the path that the operating point will follow during the 1000 hours of operation, is externally defined, as it depends on the operating point of the whole engine. The compressor operating point in such simulation tools is uniquely defined through the boundary condition of either mass flow or exit static pressure and rotational speed. As it has been shown in several cases, and experimentally proved by Tabarin [8], when fouling is present in a compressor, the pressure ratio and mass flow are in percentage equally decreased. Based on the above, the necessary boundary condition was indirectly defined as follows. An extra computational loop was added to the execution code where for each operating point the mass flow or the exit pressure, depending on whether the operating point was close to surge or stall, was progressively varied until the same in percentage reduction of pressure ratio and mass flow was detected.

Graphs on figures 1,2,3 and 4 show the decrease of pressure ratio and mass flow, as well as the decrease of the isentropic efficiency as the deposits built up with time.

Regarding the pressure ratio - mass flow variation, it is in all cases, as expected, reducing with operating time. Reduction is slightly delayed though for the cases of filtered air. Especially in the less severe of the four scenarios, the 1st one, fouling starts to have appreciable effect on mass flow and pressure ratio reduction, after the first 400 hours of operation.

Based on the graph of figure 5, it turns out that the presence of a filter has an offsetting impact on pressure ratio reduction, that is when humidity is present, pressure ratio reduction is doubling. On the other hand, according to the trends demonstrated in figure 6, humidity has a far greater impact on compressor pressure ratio reduction when the air is unfiltered, as opposed to the case where the air is filtered.

Regarding case specific pressure ratio versus isentropic efficiency reduction for unfiltered air scenarios, pressure ratio lags in reduction compared to isentropic efficiency (Figures 3,4). The exact opposite trend seems to rule in the two first scenarios where the air is filtered (figures 1,2). In particular, the relative trends spotted in the third scenario – NASA Stage 37 blades are fully fouled and the air is dry - are also verified by Melino et al. [28] who examined fouling in similar operating conditions.

Finally, in figure 7 the variation of total enthalpy rise through the compressor is plotted versus operating hours. Enthalpy rise is ruled by the pressure ratio and the isentropic efficiency. Efficiency drop leads to increased enthalpy rise whereas pressure ratio decrease causes a drop in enthalpy rise. The rates of decrease for these two parameters define the rate of change of the total enthalpy rise, which for the two-extreme scenario, 1st and 4th changes also its sign. Based on the same diagram, enthalpy rise tends to

increase with operating time when the air is unfiltered, whereas this trend reverses in the case of filtered air. Obviously, this will not lead to increased output power because the decreased pressure ratio will cause a decrease in turbine power.

Accuracy of the results is always judged against computational time consumed. The flow solution was obtained rapidly using SOCRATES in the order of minutes for a core i7 processor. This renders the current methodology applicable for optimization studies. In particular, as long as SOCRATES is integrated with a 0-D gas turbine performance simulation tool, then the hybrid calculation tool that will emerge, could introduce fouling in much greater detail, not only for optimization studies as mentioned above, but also for engine health monitoring assessment. For this type of studies, computation time consumption and correct qualitative response are the two most important characteristics. Quantitative weaknesses are to a certain extent canceled out, when similar cases are compared.

CONCLUSIONS

In the current study a streamline curvature-based flow simulation tool, was used to assess the effect of the two ruling factors of compressor fouling: i) Concentration and size of contaminants present in the incoming flow, and ii) moisture level of the air. For this study, four relevant operating scenarios were conceived and an integrated fouling loss model, developed by the authors was used. The model was extended to address the effect of degree of exposure of blades to fouling. Major findings are summarized below:

Compressor performance decrease due to increased blade surface "stickiness" is stronger compared to the corresponding decrease caused by the absence of a filter.

Moreover, in the case of unfiltered air, regardless of the blade surface stickiness level, pressure ratio decrease is smaller compared to efficiency decrease. Finally, the relevant efficiency - pressure ratio decrease, will define the sign of the enthalpy change trend over the first hours of the operation period examined. For instance, if the efficiency falls steeper compared to the MF-PR (3rd and 4th scenario) then the total enthalpy change rate is positive. In other words, the enthalpy increase due to the efficiency degradation, outbalances the enthalpy decrease due to the lower pressure ratio.

NOMENCLATURE

CFD	Computational Fluid Dynamics
REE	Radial Equilibrium Equation
SLC	Streamline Curvature
SOCRATES	Synthesis of Correlations for the Robust Assessment of Turbomachinery Engine Systems
TBO	Time Between Overhauls
CF	Coverage Factor
ω	Loss coefficient
ml	Minimum loss
OD	Off Design
p	Profile

REFERENCES

[1] Rainer Kurz, Klaus Brun, 2012, “Fouling Mechanisms in Axial Compressors” J Eng Gas Turb Power, **134**(3), pp 032401-1. doi.org/10.1115/1.4004403

[2] Templalexis I., Pachidis V., 2017, “Simulation of Fouling in Axial Flow Compressor Using a Throughflow Method”, Journal of Energy Engineering, **143**(1), doi.org/10.1061/(ASCE)EY.1943-7897.0000378

[3] Ernst Schneider, Saba Demircioglu Bussjaeger, Susana Franco, Dirk Therkorn, 2010, "Analysis of Compressor On-Line Washing to Optimize Gas Turbine Power Plant Performance" J Eng Gas Turb Power, **132**(6), pp. 500-507. DOI: 10.1115/1.4000133

[4] Meherwan P. Boyce, Francisco Gonzalez, 2007, " A Study of On-Line and Off-Line Turbine Washing to Optimize the Operation of a Gas Turbine", J Eng Gas Turb Power, **129**(1), pp 114 - 122. doi.org/10.1115/1.2181180

[5] Klaus Brun, Terrence A. Grimley, William C. Foiles, Rainer Kurz, 2015, "Experimental Evaluation of the Effectiveness of Online Water-Washing in Gas Turbine Compressors" J Eng Gas Turb Power, **137**(4), pp 042605-1,15. https://doi.org/10.1115/1.4028618

[6] Aretakis N., Roumeliotis I., Doumouras G., Mathioudakis K., 2012, "Compressor washing economic analysis and optimization for power generation", Journal of Applied Energy, **95,** pp 77-86. 10.1016/j.apenergy.2012.02.016

[7] Stalder J. P., 2001, "Gas Turbine Compressor Washing State of the Art: Field Experiencces." J Eng Gas Turb Power, **123**(2), pp 363 – 370. doi.org/10.1115/1.1361108

[8] Tarabrin A. P., Schurovsky, V. A., Bodrov, A. I., and Stalder, J.-P., 1998, “An Analysis of Axial Compressor Fouling and a Blade Cleaning Method”, J Turbomach, **120**(2), pp. 256–261. doi.org/10.1115/1.2841400

[9] Parker G. J., Lee P., 1972, “Studies of the Deposition of Sub-Micron Particles on Turbine Blades”, *Proc. Inst. Mech. Eng. Conf*., 186(38), pp. 519–526.

[10] Syverud E., Brakke O., and Bakken L. E., 2007, “Axial Compressor Deterioration Caused by Saltwater Ingestion”, J Turbomach, **129**(1), pp. 119–127. doi.org/10.1115/1.2219763

[11] Rainer Kurz, Klaus Brun, 2012, “Fouling Mechanisms in Axial Compressors”, J Eng Gas Turb Power, **134**(3), pp. 032401-1. doi.org/10.1115/1.4004403

[12] Aker G. F., Saravanamuttoo H. I. H., 1989, "Predicting Gas Turbine Performance Deterioration Due to Compressor Fouling Using Computer Simulation Techniques", J Eng Gas Turb Power, **111**(2), pp. 343-350. doi.org/10.1115/1.3240259

[13] Diakunchak I. S., 1992, "Performance Deterioration in Industrial Gas Turbines", J Eng Gas Turb Power, **114**(2), pp. 161-168. doi.org/10.1115/1.2906565

[14] Cyrus B., Meher-Homji, Mustapha Chaker, Andrew F. Bromley, 2009, "The Fouling of Axial Flow Compressor - Causes, Effects, Susceptibility and Sensitivity", *Proc of TurboExpo 2009 Glasgow, GT2009-59239, pp. 571-590*.

[15] Templalexis, I., Pilidis, P., Pachidis, V. and Kotsiopoulos, P., 2011, “Development of a 2D compressor streamline curvature code”, J Turbomach, **133**(4), DOI: 10.1115/1.2720877

[16] Pachidis V., Pilidis P., Templalexis I., Marinai L., 2008, “An Iterative Method for Blade Profile Loss Model Adaptation Using Streamline Curvature”, J Eng Gas Turb Power, **130**(1), pp 011702. doi.org/10.1115/1.2747643.

[17] Pachidis V., Pilidis P., Talhouarn F., Kalfas A., Templalexis I., 2006, “A fully integrated approach to component zooming using computational fluid dynamics”, J Eng Gas Turb Power, **128**(3), pp. 579-584. doi.org/10.1115/1.2135815

[18] Pachidis V., Pilidis P., Templalexis I., Barbosa J. and Nantua N., 2007, “A De-Coupled Approach to Component High-Fidelity Analysis Using Computational Fluid Dynamics”, Proceedings of the Institution of Mechanical Engineers, Part G: Journal of Aerospace Engineering, **221**(1), pp 105-113. doi.org/10.1243/09544100JAERO37

[19] Templalexis I, 2014, “The importance of Force Terms Modeling within the Streamline Curvature Through Flow Method” Proceedings of the Institution of Mechanical Engineers, Part A: Journal of Power and Energy, **228**(7), pp 825-835. doi.org/10.1177/0957650914539938

[20] Mirko Morini, Michele Pinelli, Pier Ruggero Spina, Mauro Venturini, 2010, "Computational Fluid Dynamics Simulation of Fouling on Axial Compressor Stages" J Eng Gas Turb Power, **132**(7), pp. 072401. doi.org/10.1115/1.4000128

[21] Koch C. C., Smith Jr. L. H., 1976, "Loss sources and magnitudes in axial-flow compressors", J. Eng. Power, **98**(3), pp 411-424. doi.org/10.1115/1.3446202

[22] Seung Chul Back, Hobson G. V., Seung Jin Song, Millsaps K. T., 2012, "Effects of Reynolds Number and Surface Roughness Magnitude and Location on Compressor Cascade Performance", J. Turbomach., **134**(5), pp 051013. doi.org/10.1115/1.4003821

[23] Aungier R. H., 2003, "Axial-Flow Compressors: A Strategy for Aerodynamic Design and Analysis", ASME Press, Three Park Avenue, New York, NY 10016, pp 177 - 197. ISBN: 9780791801925

[24] Seung Chul Back, June Hyuk Sohn, Seung Jin Song, 2010, “Impact of Surface Roughness on Compressor Cascade Performance” J. Fluids Eng., **132**(6), pp 064502. doi.org/10.1115/1.4001788

[25] Mal’tsev Y. N., Shakhov V. G., 1989, “Influence of Roughness of Deposits in Compressor Cascade on Flow Lag Angle”, Soviet Aeronautics, **32**(3), pp. 90–92.

[26] Milsch R., 1971, “Systematische Untersuchung über den Einfluss der Rauhigkeit von Verdichterschaufeln auf den Gitterwirkungsgrad”, PhD Thesis, University of Hanover, Germany.

[27] Reid L., Moore R. D., 1978, “Design and Overall Performance of Four Highly-Loaded, High-Speed Inlet Stages for an Advanced High-Pressure-Ratio Core Compressor”, NASA Report No. TP 1337, ID 19780025165

[28] Francesco Melino, Mirko Morini, Antonio Peretto, Michele Pinelli Pier Ruggero Spina, 2012, "Compressor Fouling Modeling: Relationship Between Computational Roughness and Gas Turbine Operation Time" J Eng Gas Turb Power, **134**(5), pp 052401. doi.org/10.1115/1.4004739

[29] Alessio Suman, Mirko Morini, Rainer Kurz, Nicola Aldi, Klaus Brun, Michele Pinelli, Pier Ruggero Spina, 2016, "Estimation of the Particle Deposition on a Transonic Axial Compressor Blade", J Eng Gas Turb Power, **138**(1), pp 012604. doi.org/10.1115/1.4031206

[30] Vigueras Zunica, 2007, "Analysis of Gas Turbine Compressor Fouling and Washing on Line", PhD Thesis, Cranfield University, UK.

[31] Anthony Giampaolo, 2006, "Gas Turbine Handbook Principles and Practices", CRC press, ISBN: 0-88173-516-7

[32] Urasek D. C., Gorell W. T., Cunnan W. S., 1980, “Performance of Two-Stage Fan Having Low-Aspect-Ratio, First Stage Rotor Blading”, NASA TP-1493

[33] Azamar H., Pachidis V, Templalexis I, 2017, “An Improved Streamline Curvature Based Design Approach for Transonic Axial Flow Compressor Blading”, 23rd ISABE Conference Manchester UK, ISABE-2017-22651

[34] Azamar H., Pachidis V, Templalexis I, 2017, “Development of a Streamline Curvature Axial-Flow Compressor Simulator Graphical User-Interface for Design and Research”, 23rd ISABE Conference Manchester UK, ISABE-2017-22651

Figure Captions List

Fig. 1 Compressor performance parameters variation, according to filtered - dry air (1st scenario)

Fig. 2 Compressor performance parameters variation, according to filtered - humid air (2nd scenario)

Fig. 3 Compressor performance parameters variation, according to unfiltered - dry air (3rd scenario)

Fig. 4 Compressor performance parameters variation, according to unfiltered - humid air (4th scenario)

Fig. 5 Effect of filter on PR - MF drop

Fig. 6 Effect of moisture in PR - MF drop

Fig. 7 Total enthalpy change for cleaned/fouled condition

Table Caption List

Table 1 Single-stage fan design point performance [27]

Table 2 Input Data for Fouling Scenarios

Information Regarding Figures and Tables

Table 1

Pressure Ratio	2.05
Isentropic Efficiency	0.84
Mass Flow (kg/sec)	20. 2
Rotor Tip Speed (m/s)	454

Table 2

	Description	Coverage factor	Relative surface roughness vs time elapsed.				
			200 hours	400 hours	600 hours	800 hours	1000 hours
1st	Dry filtered air	0.6	0.809	1.38	1.87	2.29	2.63
2nd	Wet filtered air	0.6	1.3	2.43	3.57	4.71	5.85
3rd	Dry unfiltered air	1.0	0.809	1.38	1.87	2.29	2.63
4th	Wet unfiltered air	1.0	1.3	2.43	3.57	4.71	5.85

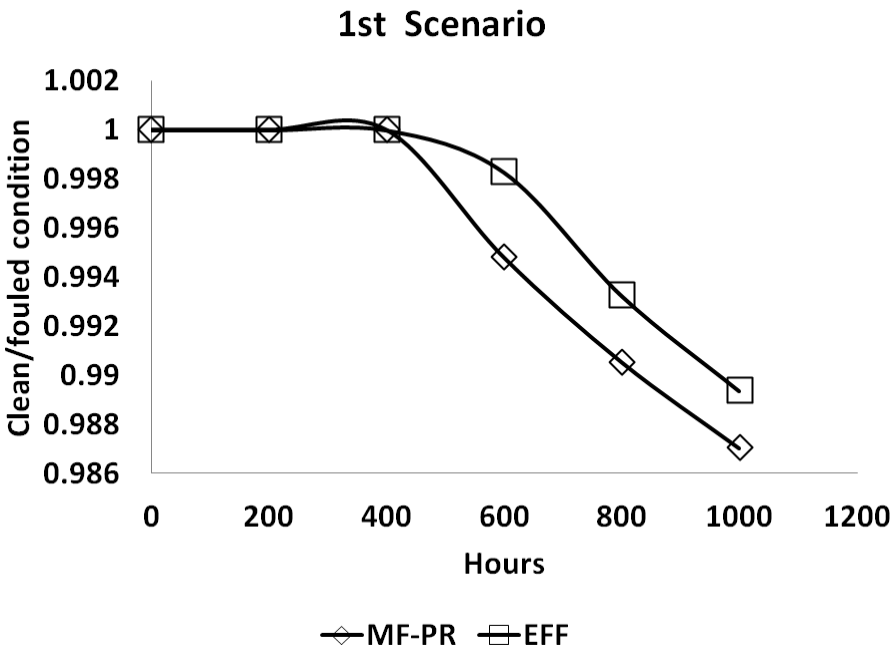


Fig. 1 Compressor performance parameters variation, according to filtered - dry air (1st scenario)

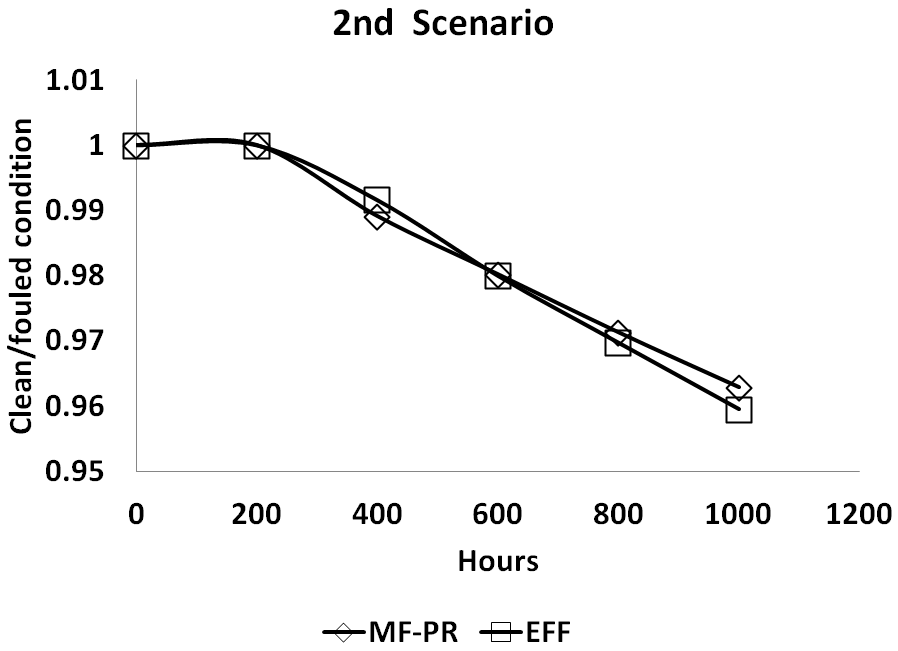


Fig. 2 Compressor performance parameters variation, according to filtered - humid air (2nd scenario)

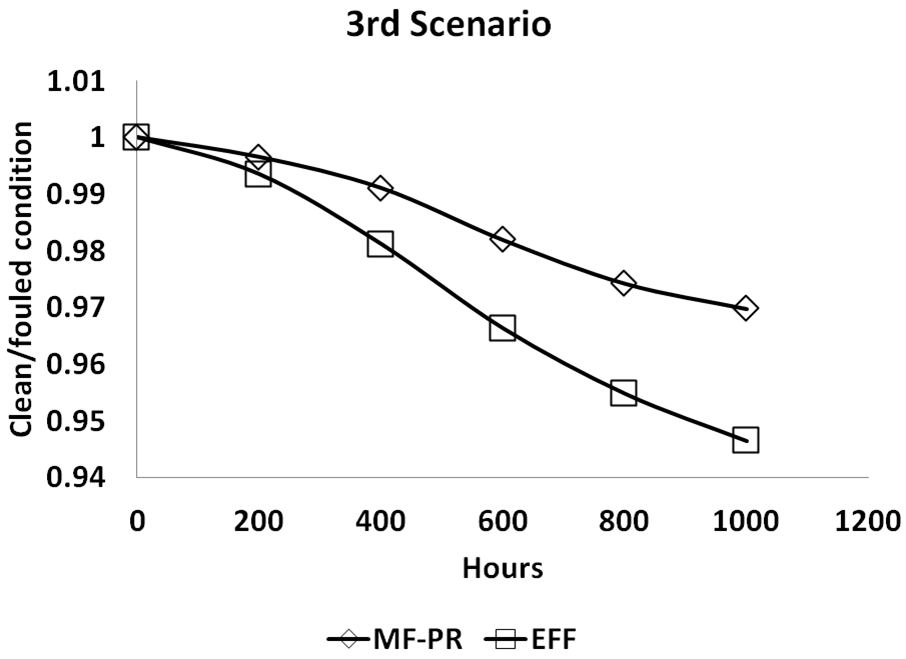


Fig. 3 Compressor performance parameters variation, according to unfiltered - dry air (3rd scenario)

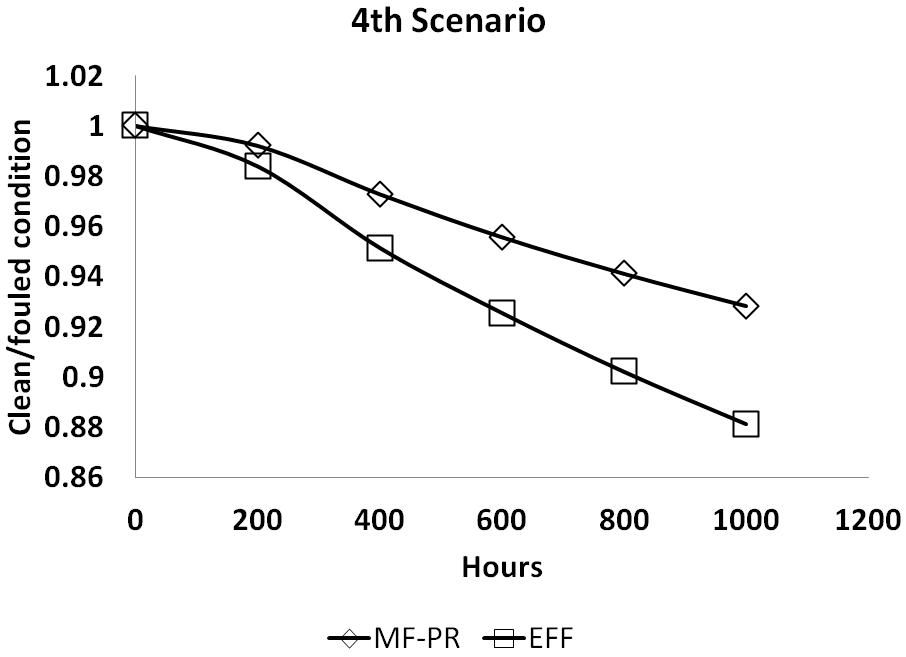


Fig. 4 Compressor performance parameters variation, according to unfiltered - humid air (4th scenario)

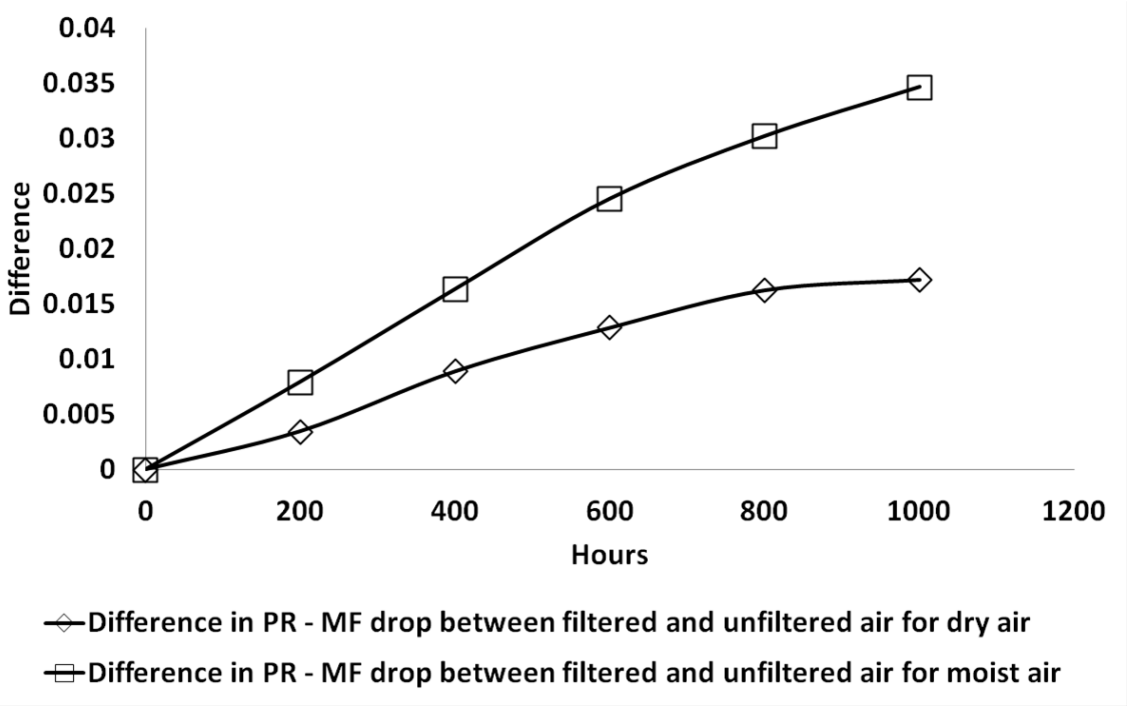


Fig. 5 Effect of filter on PR - MF drop

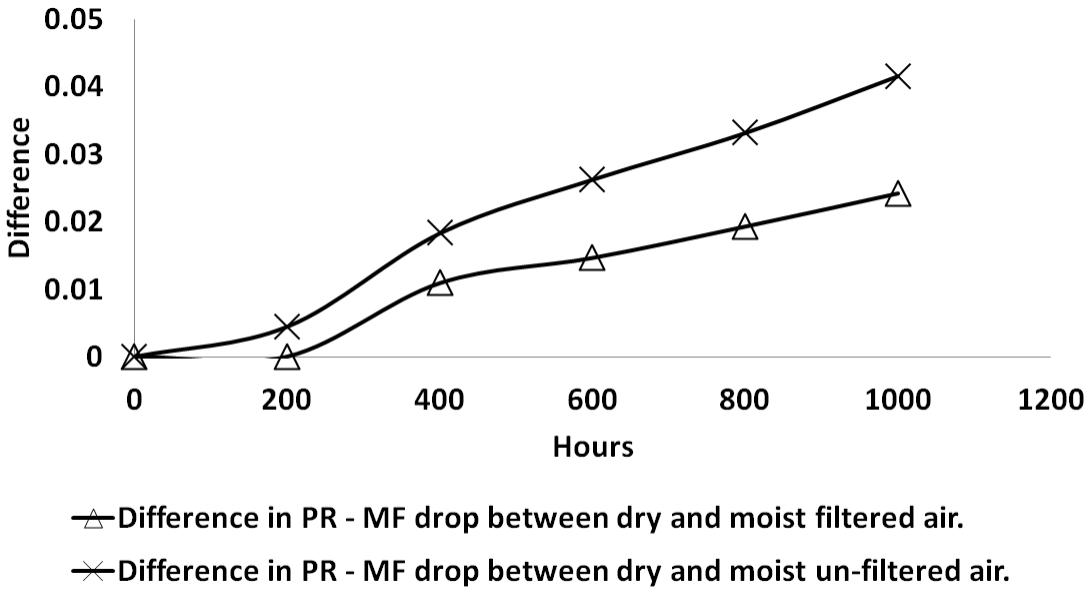


Fig. 6 Effect of moisture in PR - MF drop

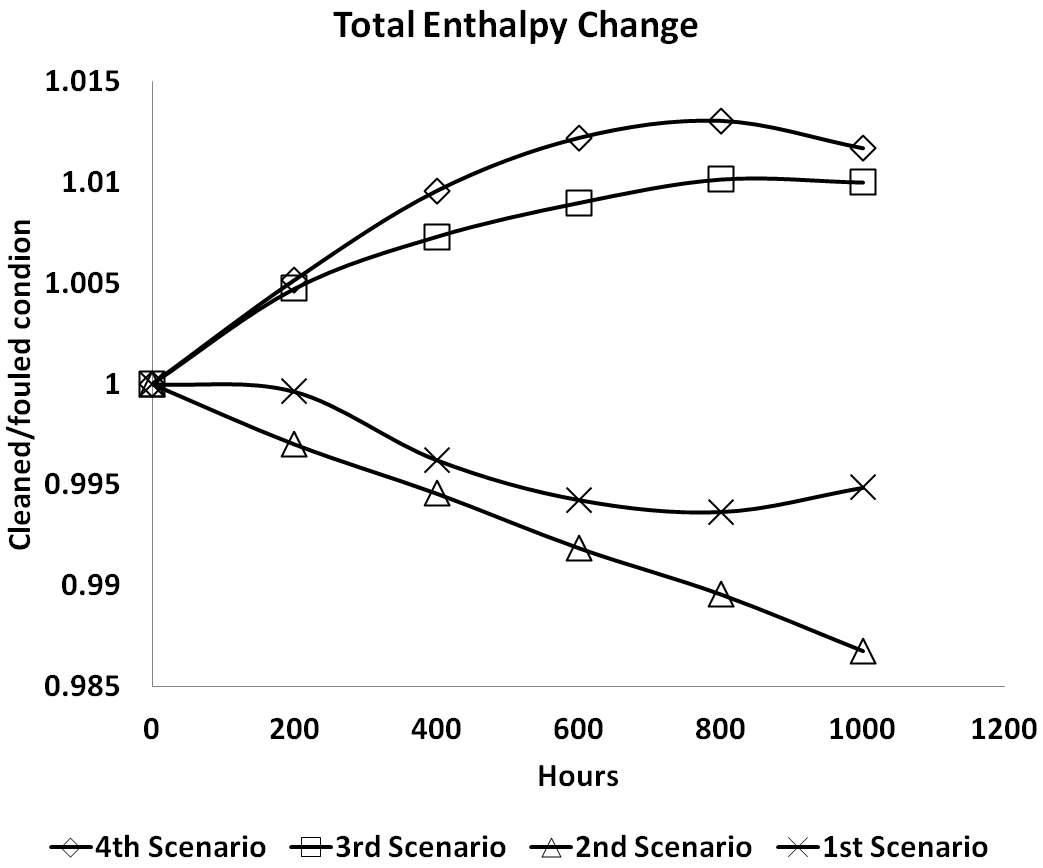


Fig. 7 Total enthalpy change for cleaned/fouled condition



https://dspace.org/

Comparative assessment of fouling scenarios in an axial flow compressor

Templalexis, Ioannis; Pachidis, Vassilios; Azamar, Hasani

2020-12-05
American Society of Mechanical Engineers (ASME)
https://doi.org/10.1115/1.4049264
Templalexis I, Pachidis V. Azamar H. (2021) Comparative assessment of fouling scenarios in an axial flow compressor. Journal of Engineering for Gas Turbines and Power, Volume 143, Issue 8, August 2021, Paper number GTP-20-1475

Downloaded from a DSpace repository. https://dspace.org/